Journal of Structural Geology, Vol. 9, No. 1, pp. 49 to 60, 1987
Printed in Great Britain

0191-8141/87 $03.00 + 0.00

Artificial generation of pseudotachylyte using friction welding apparatus: simulation of melting on a fault plane

JOHN G. SPRAY

Department of Geology, University of New Brunswick, Fredericton, Canada, E3B 5A3

(*Received* 9 *December* 1985; *accepted in revised form* 21 *March* 1986)

Abstract—A 150 μm thick fused layer of rock has been produced by rotating two metadolerite core faces against each other at 3000 r.p.m. under an axial load of 330 kg for 11 s using friction welding apparatus. Scanning electron microscopy and electron microprobe analysis reveal that the melt layer comprises sub-angular to rounded porphyroclasts of clinopyroxene, feldspar and ilmenite (<20 μm diameter), derived from the host metadolerite, set within a silicate glass matrix. Thermal calculations confirm that melting occurred at the rock interface and that mean surface temperatures in excess of 1400°C were attained. The fused layer shows many textural similarities with pseudotachylyte described from fault zones. Morphologically, the fused layer consists of a series of stacks of porphyroclasts welded together by melt to form 'build-ups' oriented at right angles to the friction surface. There is also evidence of gouging, ploughing and plucking, as well as transfer and adhesion of material having occurred between the rock faces. The mean surface velocity attained by the metadolerite (0.24 m s^{-1}) and duration of the experiment are comparable with velocities and rise times of typical single jerk earthquakes occurring during stick-slip seismic faulting within brittle crust (i.e. slip rates of 0.1–0.5 m s^{-1} for, say, 1–10 s). In these respects the experiment successfully simulated frictional fusion on a fault plane in the absence of an intergranular fluid. Power dissipation during the experiment was about 1 MW m^{-2}, comparable only to very low values for earthquakes (e.g. 1–100 MW m^{-2} for displacement rates of 0.1–0.5 m s^{-1} at shear stresses of 100–1000 bars). This indicates that melting on fault planes during earthquakes should be commonplace. Field evidence, however, does not support this contention. Either pseudotachylyte is not being recognized in exhumed ancient seismic fault zones or melting only occurs under very special circumstances.

INTRODUCTION

MELTING on fault planes due to frictional heating has been documented from a number of geological situations. Fusion products have been described from the base of major landslides, as at Langtang, Nepal, and at Kofels, Austria (Scott & Drever 1953, Erismann *et al.* 1977, Heuberger *et al.* 1984, Masch *et al.* 1985). Melt rock is also found in crustal fault zones in the form of pseudotachylyte (e.g. Jeffreys 1942, Philpotts 1964, McKenzie & Brune 1972, Sibson 1975). Some workers also believe that frictional heating on the slip zone between cold descending lithosphere and overlying mantle is responsible for partial melting and subsequent surface volcanism above zones of subduction (e.g. Turcotte & Schubert 1973), although in this case it is not possible to directly observe and sample the immediate melt products.

Melting on fault planes during earthquakes may be an important process because it has the potential to dissipate shear stress and stored strain energy during slip. Lubrication of an active fault by melt may therefore significantly increase the hazard of a seismic event. In this respect studies of the frictional characteristics of fault zones remain fundamental to understanding earthquake mechanisms. To this end investigations of natural pseudotachylytes have provided important insight into fault behaviour (e.g. McKenzie & Brune 1972, Sibson 1975). However, many pseudotachylytes from exhumed ancient seismic fault zones exhibit devitrification textures and may show the effects of subsequent metamorphism, retrogression and weathering. This altered state limits their usefulness as guides to seismogenic fault activity. As a preliminary step in attempting to further understand the process of fusion in fault zones an experiment has been conducted whereby a layer of fused rock has been artificially produced between rotating rock faces using friction welding apparatus. This approach has certain advantages over finite deformation tests (such as triaxial and simple sliding experiments) because rotary motion allows the duration of frictional heating to be varied and interface products to be studied at different stages of the experiment. It also has the advantage of producing fresh melt devoid of devitrification and secondary alteration effects.

APPARATUS AND EXPERIMENTAL PROCEDURE

Friction welding apparatus has been successfully used since the 1950s in the engineering industries to join similar and dissimilar metals or plastics by rotating one part of a material to be joined against a stationary counterpart under load until sufficient heat is generated to form a weld. In certain respects friction welding machines are similar to lathes, except that the former can rotate samples at several thousand r.p.m., deliver high axial thrusts and are designed to complete the welding cycle with a forging event (essentially a short, sharp compression). Furthermore, all these parameters can be precisely controlled according to the type of materials being welded. One of the components to be joined has to be of a round or regular shape (i.e. bar, square, tube or hexagon tube), whilst the other can be of

any configuration provided it is held securely and presents a butt face. The welding cycle commences with one of the materials being rotated then brought into contact with its counterpart under a pre-determined axial load. Rubbing and wear occur between the two abutted faces which break down surface contamination and create clean surfaces. As the interface temperature rises due to the frictionally generated heat, the material becomes plastic and a weld begins to form. For industrial applications a forging force is applied at the end of the heating cycle after rotation has ceased to ensure that a complete bond is formed; excess weld material being extruded around the components' edges. The technique is used to join, for example, railway wheels to axles, high strength bearing housings to axle casings on road vehicles, internal combustion engine valve stems to valve heads and the plastic hemispheres of fishermen's floats. There now exist numerous variations of the process including continuous and inertia drive machines with axial, orbital or radial capabilities.

The experiment was performed at the Welding Institute, Abington, Cambridgeshire, U.K. The apparatus used was an FW7 continuous drive orbital friction welding machine which was built in the mid-1970s by the Friction Welding Company as a development tool (Fig. 1). It possesses a transmission power rating of 35 kW, develops a maximum axial thrust of 100 kN and a maximum rotating speed of 3000 r.p.m. Orbital machines are unusual in their ability to drive the samples off-axis; the FW7 having an offset range of 1–3 mm. Samples are held within the drive spindles by tapered collets and, unlike the more conventional axially driven friction welding rigs whereby one of the samples is held stationary, the orbital machine is geared to drive both spindles in unison (Appendix 1). This design feature was conceived to facilitate the joining of square bars by maintaining a constant angular relationship during rotation. Frictional heat is generated due to the offsetting of the sample axes and is produced evenly over the rubbing interface, in contrast to axial rotation whereby heat generation at the axis is negligible. The drive spindles are powered hydraulically via an electrically driven pump (Fig. 1).

With regard to rock sample preparation, a 20 cm long section of metadolerite was taken from a 3.15 cm diameter core sample penetrating the lower levels of the Skaergaard intrusion. The section was then carefully cut at right angles to its length using a diamond saw to produce two 10 cm long cylinders. The faces of the cylinders were polished on wetted glass with F800 'Aloxite' powder in a similar manner to that used for thin section preparation (Fig. 2a). This was done to eliminate gross surface irregularities due to the saw-cutting. Each rock cylinder was then sleeved in a mild steel support tube and loaded into the two collets of the welding machine (Fig. 2b). Their faces were then rotated against each other for 11 s, at 3000 r.p.m., an orbital offset of 0.0015 m (equivalent to a mean slip rate of 0.24 m s^{-1}; Appendix 1) and an axial loading of 330 kg. This is equivalent to an axial force of about 4500 kg m^{-2} (Appendix 2) and a mean surface pressure of 50 bars or 5 MPa. For the purposes of this work the final forging facility was not used.

RESULTS

The operating conditions were monitored during the experiment and a graph output was produced via an online computer. This is shown in Fig. 3. The total 'start run' to 'end run' time was 12.5 s; the last 1.5 s being taken up by braking the drive spindles to a stop, resulting in a total heating time of 11 s. It can be seen that the spindle speed gradually increases and the torque gradually decreases during the heating cycle (Fig. 3). There was negligible axial shortening. The orbit value (axial offset) was pre-set at 0.0015 m.

Macroscopic observations

During the first 2–3 s of the experiment the interface was observed to partly spall and dust was produced. Spalling occurred at the edges of the unprotected core faces where they protruded from the support sleeves. The interface glowed cherry red for the remaining 8–9 s and a burnt rock smell was created. Following the experiment it was observed that a sliver of metadolerite had been transferred from one face to the other (Fig. 4a). A matt black fused layer, up to 150 μm thick, had been produced, which partly covered both core sample faces and appeared to bond the transferred sliver. A pale grey powder (gouge) comprising fine rock particles and rock dust also partly covered both faces and was particularly thick on one face (Fig. 4b).

Microscopic observations

Scanning electron microscope photomicrographs of a polished section cut normal to the edge of one of the metadolerite faces are shown in Figs. 5(a)–(f). The sample shows a section from metadolerite through the fused layer to an attached metadolerite sliver which was plucked and transferred from the opposing face during the experiment. The photographs were taken in back-scattered electron mode. Under these operating conditions mineral phases that are normally light coloured (e.g. feldspar) appear dark and, conversely, dark minerals (e.g. pyroxene, amphibole, opaques) appear light. Figure 5(a) is an overall view of the section, which is up to 750 μm thick. The lower 550 μm portion was deliberately chipped from one of the metadolerite faces after the experiment. Above this is the <150 μm fused layer to which is stuck the 100 μm sliver of transferred metadolerite. Fractures can be seen running sub-parallel to the original face, as can a post-experiment joint cutting both the outer sliver and fused layer at a high angle. Figures 5(b) and (c) are more detailed views of the fused layer. It mainly comprises sub-angular to rounded porphyroclasts derived from the host metadolerite faces ('wallrock') set in a sub-microscopic matrix. There is a

Fig. 1. Model FW7 continuous drive, orbital friction welding machine (total height about 1.5 m). Drive spindles can be seen at the top centre of the machine, below uplifted protection shield. Controls and computer print-out are at extreme left.

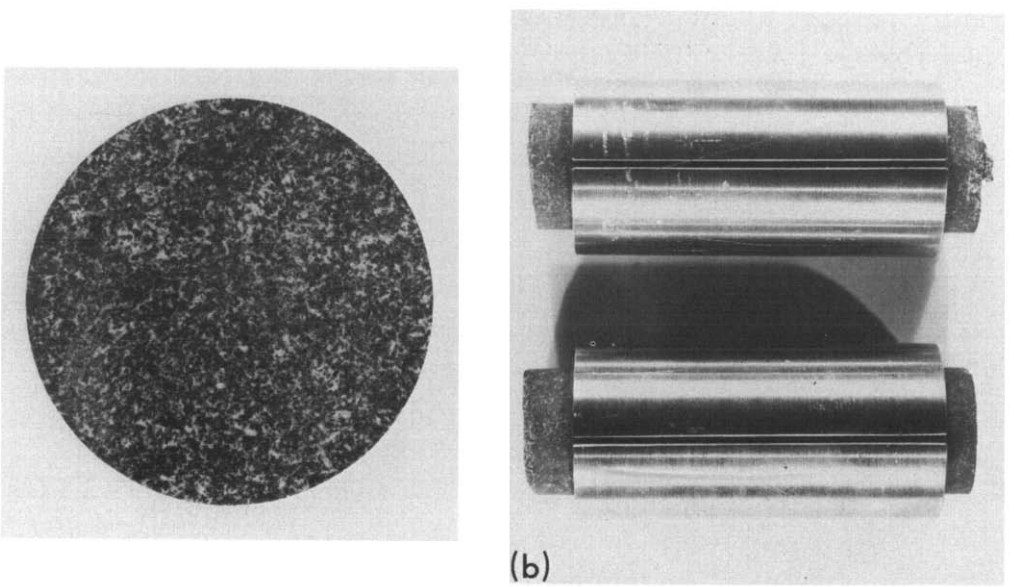

Fig. 2. (a) Polished 3.15 cm diameter face of core of metamorphosed dolerite shown prior to the experiment. Light areas: feldspar; dark areas: mainly pyroxene, amphibole and ilmenite (see text for details). (b) Side view of dolerite samples sleeved in mild steel support tubes; after experiment. The right-hand end of the upper sample shows a fragment of dolerite transferred from the opposing face and adhering via a thin black layer.

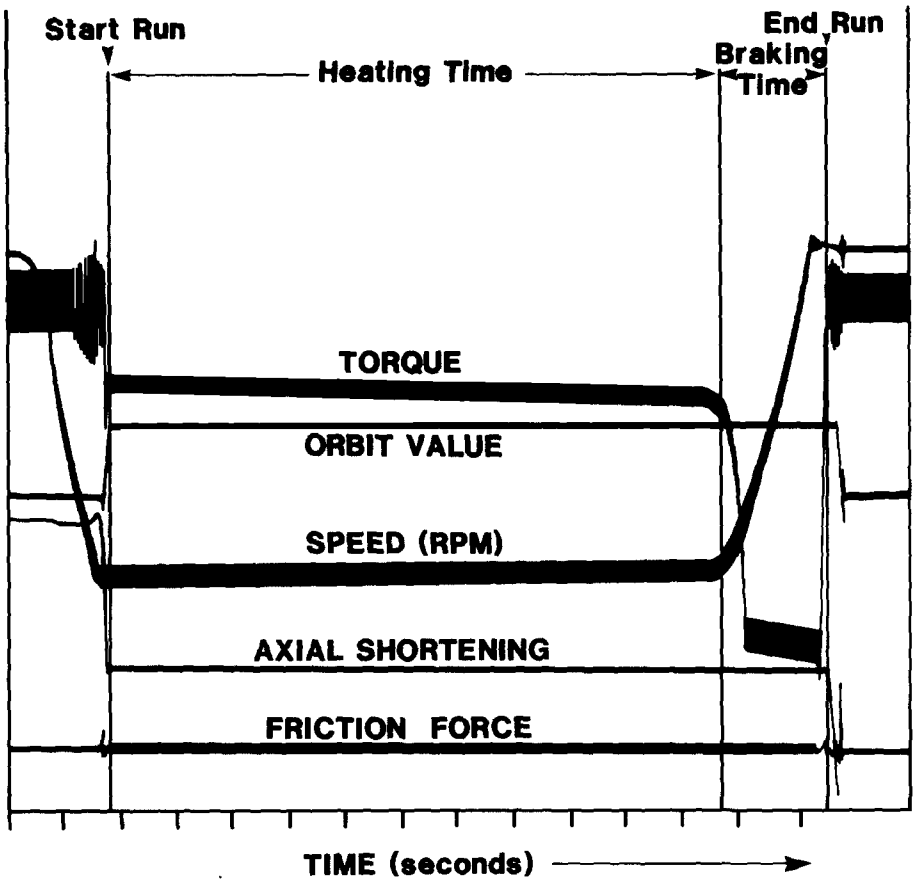

Fig. 3. Relative operating conditions of the friction welding apparatus during the experiment. Note that the torque shows a slight decrease and speed a slight increase during the heating time.

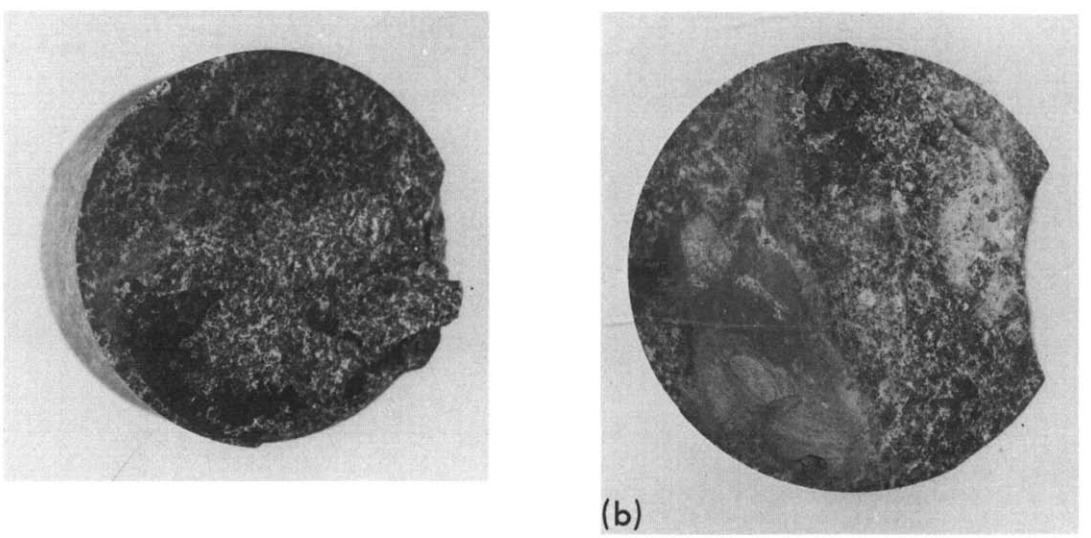

Fig. 4. (a) Oblique view of one dolerite face after the experiment (3.15 cm diameter). Note the presence of a black layer and adhered fragments of metadolerite from the opposing face. Part of the edge has spalled off. (b) Opposing face to (a) (same diameter but photographed in plan). Note the presence of fine grey powder (gouge), black layer and missing edges due to spalling.

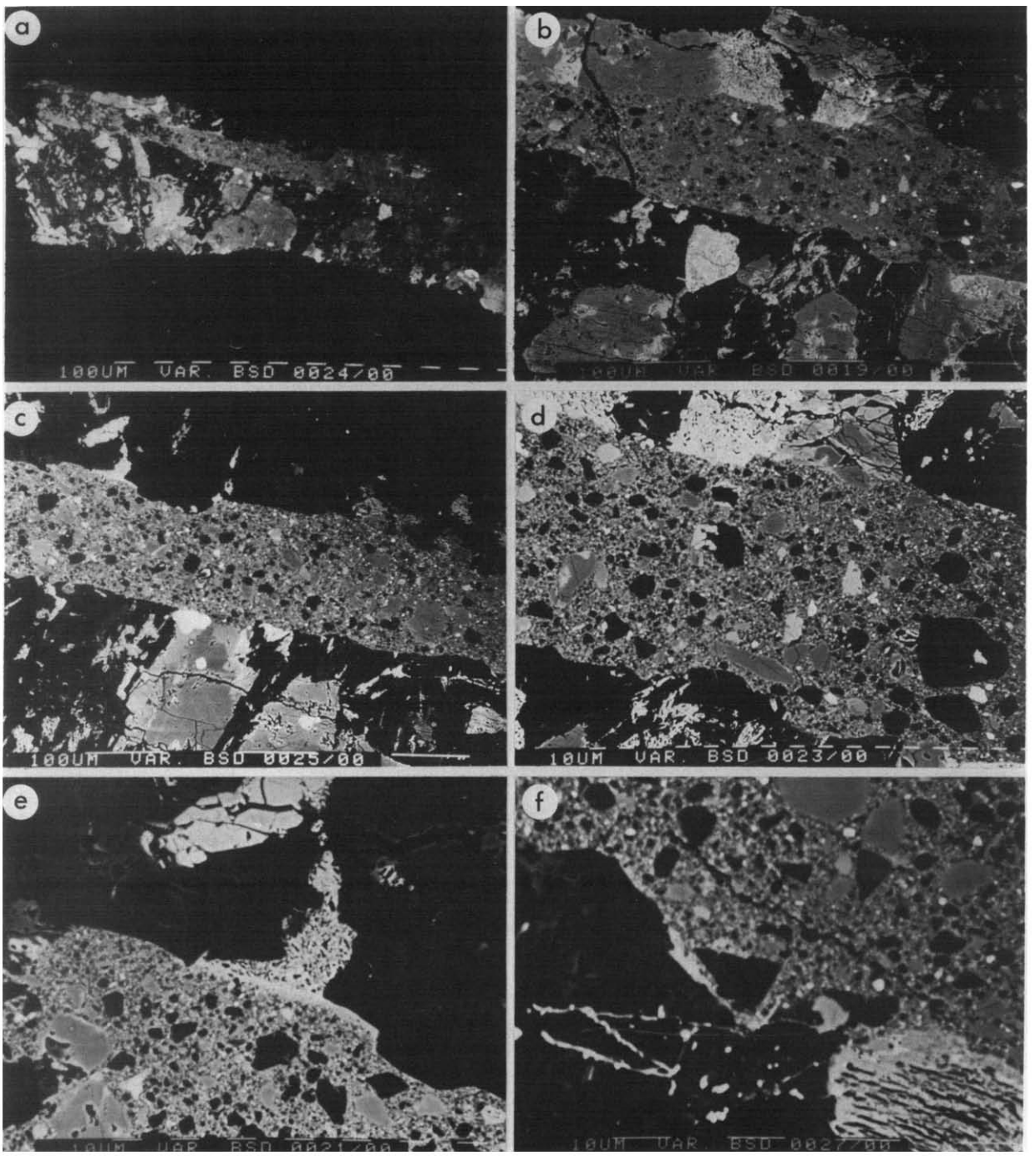

Fig. 5. Backscattered SEM photomicrographs of a polished section cut from the edge of one of the dolerite faces through the black layer to the adhering fragment transferred from the opposing face (see Figs. 2b and 4a). Scale indicated in μm by dashed white lines at the base of each photograph. (a) Overview of sample showing the fused layer (up to 150 μm thick) with thin adhering fragment adjoined (top). (b) Enlargement showing the fused layer comprising porphyroclasts set within a matrix. The grain size of the dolerite protolith is greater than that of the porphyroclasts in the fused layer. Dark grains: feldspar; light grains: pyroxene, amphibole and ilmenite. The transferred fragment and fused layer are both cracked by a post-experiment 'cooling joint'. (c) Fractures within the protolith can be seen trending sub-parallel to the fused layer. (d) The porphyroclasts are predominantly sub-angular to rounded and, in places, are composite. (e) Note the relatively smooth but curved edges of the 'fault' wall and the way melt has exploited fractures. (f) The dark triangular-shaped clast (?feldspar) in the centre of the micrograph appears to have been frozen in position immediately after its release from the fault wall.

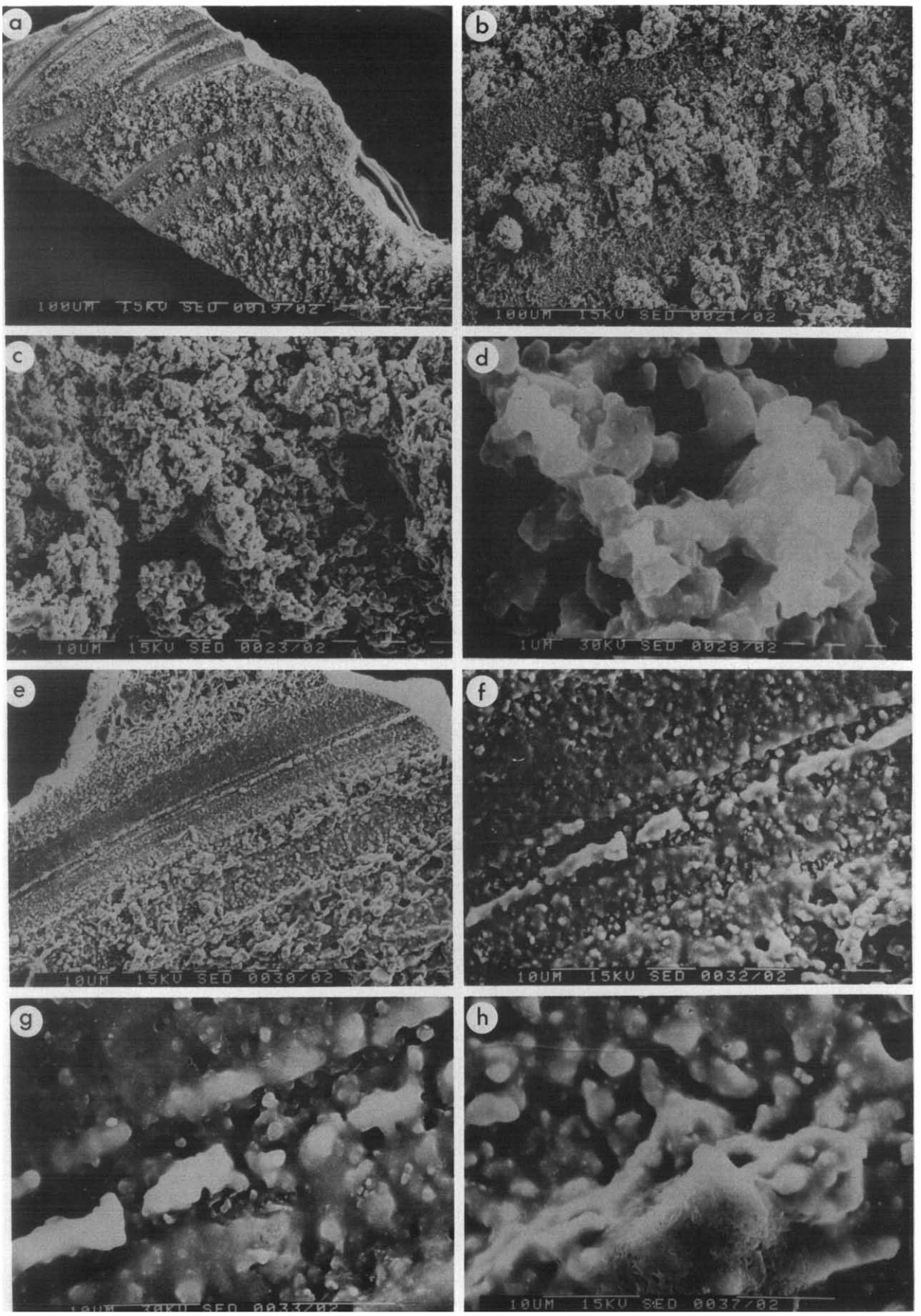

Fig. 6. (a)–(d) SEM photomicrographs showing pseudotachylyte morphology in areas of overall positive relief ('build-ups') at increasing scales of magnification (see text for details). (e)–(h) SEM photomicrographs showing pseudotachylyte morphology in areas of overall negative relief (plough regions) at increasing scales of magnification (see text for details). Scale indicated in μm by dashed white lines at the base of each photograph.

wide range in size of the porphyroclasts, but all appear considerably smaller than the original grains in the host metadolerite. Some of the porphyroclasts are composite, but the majority are monomineralic (Fig. 5d). Despite face polishing, the microscopically uneven profile of the metadolerite faces can be seen in all photomicrographs, especially Figs. 5(e) & (f). There is evidence that the melt phase has exploited or even created fractures in the wallrock such that material has become detached from the metadolerite faces and incorporated into the fused layer. This is illustrated in Fig. 5(f) where a dark (feldspar), triangular-shaped fragment became frozen in the process of being removed from the wall at the very end of the experiment.

Gold coated but otherwise unprepared fragments of the fused layer were also examined in plan view under the SEM (Figs. 6a–h). Figure 6(a) is an overall view of one particular fragment. The most striking feature of the surface morphology is its relative roughness and complexity. Lumpy clots of material, between which occur irregular spaces and cavities, are accompanied by scored indentations of broadly concentric form, some of which disappear in the middle of the fragment rather than its edge. The surface morphology can thus be divided into two distinct types: (1) accumulated aggregates of material, with overall positive relief, which will be referred to as 'build-ups' and (2) indented, or ploughed regions, with overall negative relief.

Figures 6(b)–(d) show an area of 'build-ups' at progressively increased magnification. It is clear that they are composite and comprise welded aggregates of clasts (presumably the porphyroclasts seen in section in Fig. 5). The 'build-ups' form columnar structures with their diameter (20–100 μm) being less than their height (100–150 μm). They do not appear aligned in any preferred direction and the size of the constituent clasts is variable (Fig. 6d). Major contrasts in relief are indicated by dark areas immediately adjacent to certain 'build-ups' (Figs. 6c & d). In Figs. 6(c) & (d) it is apparent that the clasts are set in a matrix which shows no evidence of crystallinity but has features indicative of a melt, as suggested by smooth rounded edges. Figure 6(d) shows that the 'build-ups' themselves contain structural cavities. Small fragments (whiter areas) can also be seen within the translucent glassy matrix. The 'build-ups' show certain features in common with 'welded clumps' produced in sliding-friction experiments on sandstone by Friedman *et al.* (1974) and with 'moss' and 'pebble' frictionites generated from quartzo-feldspathic augen gneiss in the experiment of Erismann *et al.* (1977).

Figures 6(e)–(h) show an area of 'plough' features at progressively increased magnification. Figure 6(e) is the top corner of the same fragment shown in Fig. 6(a). In general the ploughed areas comprise finer grained clasts and a greater amount of glass than do the 'build-up' areas, although 'build-up'-like structures do occur on the ploughed valleys. These, however, possess smaller height to diameter ratios than their more columnar counterparts. Figure 6(f) shows a relatively flat ploughed 'valley' with two narrow (<10 μm wide) discontinuous concentric beads of material running along its centre. The concentric beads clearly possess glassy textures (Figs. 6g & h). Figure 6(h) shows part of a bead segment in detail. Its surface is pitted with 'vesicles' (<1 μm in diameter). The amorphous shape and translucent appearance of the surface are indicative of melt-textures.

Chemistry

The metadolerite sample used in the experiment is a medium-grained metamorphosed clinopyroxene–plagioclase–ilmenite assemblage with secondary brown amphibole, chlorite, epidote, albite and sphene. The rock is massive with no evidence of a tectonic fabric. Retrogression of the dolerite appears to have proceeded in two stages: a high temperature hydration event corresponding to the formation of pleochroic brown amphibole after clinopyroxene and a lower temperature effect concomitant with the saussuritization of plagioclase, formation of chlorite after amphibole, sphene after ilmenite and crystallization of vein epidote. Compositions of primary and secondary phases are shown in Table 1. The clinopyroxene is an augite. Virtually all plagioclase has been altered to albite. The amphibole is a tschermakitic hornblende and is unusual in its high Na and Ti contents. Combined with the high Al^{IV} and

Table 1. Electron microprobe analyses of primary and secondary mineral phases from the metadolerite, and of glass from the artificially produced pseudotachylyte. The total weight % for sphene includes 0.21% Cr_2O_3. The ilmenite–sphene grain analyzed is highly altered, resulting in the low total. Glass I approximates the amphibole composition (see Fig. 7). Glass II shows higher Al_2O_3 and Na_2O, indicating that albite has also been assimilated into melt. Glass I and II totals include 0.19% P_2O_5

	Augite	Albite	Ilm–Sph	Amphib	Chlor	Epid	Sphene	Glass I	Glass II
SiO_2	50.30	68.28	15.01	43.72	25.38	37.86	29.97	47.90	48.27
TiO_2	1.06	0.00	19.57	2.77	0.00	0.00	33.99	1.87	2.09
Al_2O_3	3.44	19.76	0.96	9.20	19.16	21.93	3.43	11.58	14.84
FeO*	9.96	0.43	45.08	17.53	36.71	15.47	1.20	14.09	13.04
MnO	0.29	0.00	0.00	0.36	0.44	0.27	0.00	0.23	0.00
MgO	13.18	0.00	0.00	10.90	8.40	0.00	0.00	6.89	5.09
CaO	21.55	0.38	13.60	10.77	0.11	22.64	28.23	11.69	10.42
Na_2O	0.00	11.81	0.00	2.41	0.00	0.00	0.00	2.92	4.07
K_2O	0.00	0.09	0.00	0.75	0.00	0.00	0.00	0.63	0.74
Total	99.78	100.75	94.22	98.41	90.20	98.17	97.03	97.99	98.75

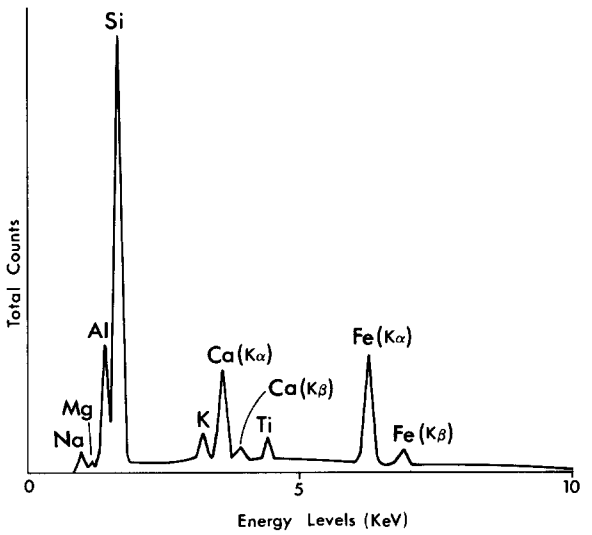

Fig. 7. SEM/microprobe X-ray spectra for the glass matrix of the artificially produced pseudotachylyte. Its profile shows a close resemblance to that of an amphibole.

relatively low Si, a high temperature origin is indicated (e.g. Raase 1974).

The fused layer comprises porphyroclasts of the metadolerite phases, mainly clinopyroxene, albite and ilmenite with the glass matrix having an 'amphibolitic' composition (Table 1, Glass I; Fig. 7). There is also evidence that some albite has been preferentially assimilated into the melt (Table 1, Glass II). Significantly, no clasts of amphibole were found in the fused layer. The preferential melting of hydrous phases during the mechanical breakdown and disruption of mineral lattices has been reported in natural pseudotachylytes (e.g. Allen 1979), and this appears to be supported by the composition of the matrix of the artificially produced pseudotachylyte.

INTERPRETATION

Applicability of friction theory

Although largely based on studies of metals, the classic friction experiments of Bowden & Tabor (1954, 1964) have thrown considerable light on the sliding behaviour of rock in the upper parts of the lithosphere. For example, the concept of stick-slip motion has been applied to the movement of faults and is widely held to be responsible for the generation of shallow focus earthquakes (Brace & Byerlee 1966). It is of interest, therefore, to see how the textures and structure of the experimentally produced fused rock layer compare with the products of conventional sliding experiments. One obvious difference is that friction welding apparatus provides rotary motion such that the same two areas of 'fault' plane remain in constant contact. Furthermore, the movement of a mineral clast lodged between faces moving in orbital motion will not be circular, but will involve a complicated trajectory and varying velocity. In this respect friction welding apparatus does not provide a simple analogue for unidirectional sliding on a fault plane.

The two basic laws of friction show that frictional resistance is (i) proportional to the load and (ii) is independent of the area of the sliding surfaces. The second law arises from the fact that all apparently flat surfaces possess irregularities, no matter how carefully prepared, and as a result the real area of contact is limited to the tips of topographic highs or asperities. Overcoming the frictional resistance is then dependent on climbing over or breaking asperities. It is also dependent on overcoming the strong adhesion which may have developed between asperity tips. Adhesion in metals is caused by the development of intermetallic junctions at the points of real contact (i.e. a form of 'cold weld'), but it is not clear whether such processes occur between silicates in fault zones. A further contribution to frictional resistance comes from the indentation and ploughing of hard asperities into a softer substrate. Because of the composite nature of rock and differences in hardness shown by different minerals, there would appear to be considerable potential for the development of plough features during faulting. Slickensides may be considered one example. Plough features are clearly present on the surface of the artificially produced fused layer (Figs. 6e–h). The grooves show finer-grained textures and a greater development of melt than those areas showing 'build-up' morphology (Figs. 6a–d). This indicates that more energy has been expended, and presumably more frictional heat has been generated, where asperities have ploughed through the surface, that is at the real points of contact.

Static frictional resistance (μ_s) is believed to be due to the force required to break locked asperities, while the subsequent onset of sliding leads to an increase in real area of contact with time and a changing kinematic frictional resistance (μ_k) until asperity locking occurs and the process repeats itself. Polished sliding surfaces that have undergone this type of stick-slip motion typically show 'carrot'-shaped plough features formed by asperity indentation (Scholz & Engelder 1976). The narrow ends of the 'carrot' grooves point in the direction of motion of the grooved surface and mark the start of the indentation process. These features were also generated during the experiment and can be seen in Figs. 6(e) & (f). Asperity ploughing and eventual failure may also account for the origin of the transferred metadolerite sliver (Fig. 4a). This may have started as an asperity which subsequently ploughed into the substrate until it became locked and sheared off as a fragment which then adhered to the opposing face via the intervening fused layer. Such plucking, transfer and adhesion of rock slivers may have occurred several times during the rotation period.

Comparisons with natural pseudotachylyte

There is some debate as to whether all so-called pseudotachylytes have undergone fusion (e.g. Shand

1916, Reynolds 1954, Philpotts 1964, Wenk 1978), but it has been conclusively shown, from detailed studies of textures and vein geometries of certain pseudotachylytes and from theoretical considerations of frictional heat generation, that melting on fault planes due to fault movement can and does take place (e.g. McKenzie & Brune 1972, Sibson 1975, Allen 1979, Grocott 1981, Maddock 1981). Fused rock produced in this way is typically very hard, extremely fine grained, glassy, dark and opaque and often contains rounded rock fragments (collectively termed quasi-conglomerates). Microscopic observation reveals devitrification, flow, spherulitic and microlitic textures.

In many respects the fused layer produced by the friction welding experiment is comparable to a pseudotachylyte. The absence of microlites and spherulites may be due to the rapid cooling of the comparatively thin melt layer (<150 μm). The rounding of wallrock clasts in natural pseudotachylytes has been attributed to three main processes (Sibson 1975): (i) attrition caused by rotational grinding; (ii) explosive decrepitation due to fluid expansion during rapid heating; and (iii) thermal corrosion by the melt phase. It is likely that all three processes played a role in the formation of the predominantly sub-angular to rounded porphyroclasts produced in the artificial pseudotachylyte (Figs. 5a–f). In particular, the breakdown of amphibole during frictional heating and its preferential incorporation into the melt phase would have released H_2O, causing fluid expansion and a transient hydrostatic pressure increase. Such overpressures were probably responsible for crack penetration by the melt phase and the consequent plucking and release of wallrock material (Fig. 5f).

Development of the fused layer

Although it is the investigation of the end product of the frictional heating episode that forms the basis of this particular experiment, a sequence of events leading up to the development of the fused layer can be envisaged.

Initial contact under rotation and load is considered to have involved crushing, grinding, attrition and surface gouging due to the interaction of the microscopically uneven rock surfaces. These processes would have dominated the first 3 s of contact during which time the spalling of cylinder faces and generation of rock dust was observed. No interface glowing took place and temperatures are considered to have been relatively low. Gouge production would have been the dominant interfacial process.

Continued rotation would have led to an increase in mechanical breakdown of mineral porphyroclasts and a progressive increase in temperature. At this stage it appears that it was the hydrous phases (mainly amphibole) which were the most susceptible to melting, resulting in the 'glueing' and coagulation of groups of predominantly anhydrous porphyroclasts. Further rotation would have lead to the mechanical attrition, thermal corrosion and explosive decrepitation of the remaining anhydrous porphyroclasts and their partial assimilation into the melt, so modifying its composition from amphibole-dominated towards bulk rock (metadolerite).

As soon as melt formed the frictional resistance would have dropped and less heat would have been generated. Because of this the melt would have frozen and continued rotation would have involved mechanical disruption of the pseudotachylyte layer followed by renewed gouge formation and a repeat of the process. Repetition of the sequence 'mechanical breakdown → heating → melting → freezing' would have occurred many times during the 8–9 s period when the interface glowed cherry red. It is by this process that the 'build-ups' are believed to have developed: layer upon layer of melt-enclosed porphyroclasts being accumulated at each successive melting event followed by their partial destruction during a cooler attrition period. Plough features are also likely to have been created and destroyed several times during the experiment: those remaining having been formed towards the very end of the 11 s cycle. At any given moment during glowing it it also likely that melting and gouge formation were occurring simultaneously in different regions of the interface. This is difficult to verify, but is supported by the coexistence of pseudotachylyte and gouge on the surfaces of both rock faces at the end of the experiment.

DISCUSSION

The conditions under which the artificial fused layer was produced are comparable, at least in terms of velocity and duration, to those prevailing during certain large earthquakes (Table 2). The conditions of the experiment are also broadly comparable in terms of power dissipa-

Table 2. Comparative source parameters for selected earthquakes and friction welding experiment

Earthquake	Magnitude	Stress drop (bar)	Mean slip (cm)	Duration (s)	Velocity ($cm\,s^{-1}$)	Reference
This experiment	?	?	264	11	24	This work
Nishi-Saitama, Japan (1931)	7.0	43	100	2	50	Abe (1974a)
Tottori, Japan (1943)	7.4	83	250	3	42	Kanamori (1972)
Fukui, Japan (1948)	7.3	83	200	2	100	Kanamori (1973)
Wasaka Bay, Japan (1973)	6.9	32	60	2	30	Abe (1974b)
Gibbs II, Mid-Atlantic Ridge (1974)	6.9	?	180	10	18	Kanamori & Stewart (1976)
Campania–Lucania, Italy (1980)	6.9	35	170	6	28	Deschamps & King (1983)

tion: for a likely static coefficient of friction (μ_s) of 0.75 for the metadolerite (Byerlee 1978) under a normal stress (σ_n) of 50 bars during the experiment, the shear stress (τ) is estimated to have been 37.5 bars (from $\tau = \mu_s \sigma_n$). This gives an average power dissipation (Q) of 0.9 MW m^{-2} (from $Q = \tau v$, where v is mean surface velocity). For natural faulting, sliding at constant shear resistances of 100–1000 bars at velocities of 10–100 cm s^{-1}, power dissipation in the range 1–100 MW m^{-2} is considered likely (Husseini 1977, Scholz 1980, Sibson 1980). Energy production for the experiment therefore appears to have been analogous to conditions of rather low-stress faulting ($\tau \leq 100$ bars). Simple thermal calculations (Appendix 3) indicate a mean surface temperature rise at the interface of at least 1400°C. Higher temperatures are likely to have been realized at the real points of contact. These temperatures would have resulted in the melting of most of the mineral phases in the metadolerite, even at atmospheric confining pressure. Lubrication of the sliding interface by melt may account for the slight reduction in torque and slight increase in speed (r.p.m.) recorded during the experiment (Fig. 3). However, virtually no change in the friction force was noted, which does not lend support to the proposal that melting on fault planes may facilitate the release of almost all the elastic strain (cf. McKenzie & Brune 1972). More work is required to verify this observation.

Pseudotachylyte has been artificially generated with relative ease, yet under shear stress considerably less than that purported to prevail during large earthquakes. It is therefore difficult to escape the conclusion that pseudotachylyte should be extremely common in fault zones which have been seismically active. However, field studies do not support this contention. Pseudotachylyte, if present at all, is normally found in quantities significantly subordinate to cataclasite and mylonite (e.g. Higgins 1971). There are a number of possible explanations to account for the apparent scarcity of pseudotachylyte: (1) failure to recognize pseudotachylyte in the field; (2) destruction due to subsequent cataclastic and/or mylonitic fault movements; (3) effect of pore-fluid pressure; (4) absence of a hydrous mineral phase in the wallrocks; and (5) displacement occurring on numerous faults rather than on a single fault.

Underestimation of the true abundance of ancient exhumed pseudotachylyte may be due to devitrification of melt glasses, subsequent metamorphism, retrogression and weathering making its recognition difficult. While such an underestimation is possible, it seems an unlikely explanation to account completely for the general scarcity of pseudotachylyte.

It is possible that certain pseudotachylytes have been reworked into cataclasites and/or mylonites by subsequent faulting occurring at lower velocities and/or lower shear stresses, such that fusion temperatures were not reached. Large earthquakes followed by smaller earthquakes on a common fault plane could provide the conditions for pseudotachylyte destruction. However, such reworking is unlikely to completely obliterate pseudotachylyte, especially injection veins which typically intrude country rock some distance from the fault. Furthermore, as the glassy nature of many pseudotachylytes necessitates near-surface cooling, subsequent deformation is also likely to be high level and consequently brittle rather than ductile.

The role of pore-fluid pressure in modifying frictional resistance during faulting has been discussed by a number of workers (e.g. Sibson 1973, Lachenbruch 1980). Frictional heating would tend to expand pore fluid and cause a transient pressure increase. This could induce a sharp decrease in both the effective normal stress and dynamic friction on the fault surface. The effectiveness of this process would depend on the presence of sufficient pore fluid, the degree of wallrock permeability, the rate of pore dilation and the width of the shear zone. Frictionally induced pore-fluid pressure could reduce the potential of a moving fault to generate heat. Such an explantion has been proposed to account for the lack of a thermal anomaly around the San Andreas fault zone (Lachenbruch & Sass 1980). 'Dry' faulting (in the absence of an intergranular fluid) would therefore tend to favour greater frictional heat generation, while 'wet' faulting would not. In this respect the friction welding experiment represents a dry-faulting analogue.

Allen (1979) has suggested that melting during faulting occurs preferentially in crystalline quartzo-feldspathic rocks possessing both high shear strengths and a significant water content contained within a hydrous mineral phase. The metadolerite sample used for the experiment is clearly not quartzo-feldspathic, but it does possess a relatively high water content which is mainly carried by amphibole. The presence of water is critical to melting because it effectively lowers the temperature of fusion, lowers viscosity and acts as a catalyst. Water-assisted melting would explain the preferential assimilation of amphibole into the artificial pseudotachylyte matrix because, during progressive grain size reduction, hydrous phases would melt first. The role of chemically bound water in assisting fusion is borne out by the absence of pseudotachylyte in faulted granulite facies anhydrous rocks (Wenk 1978). Recent studies by Chyi *et al.* (1985) also indicate that the mechanical anisotropy of certain minerals (e.g. amphibole, feldspar) may facilitate preferential disaggregation and melting (Table 1, Glasses I & II). These observations emphasize the non-equilibrium nature of melting caused by frictional heating on fault planes.

It is known that displacements in nature are commonly taken up by numerous faults or crush zones rather than by a single fault. In this respect many fault zones cannot be modelled by simple single jerk analogues (King 1978). Because of this any given fault within such an active fault zone may undergo only very short duration slip and so generate insufficient heat to cause melting. Consideration of the effects of slip across a zone of finite width rather than on discrete sliding surfaces is also important. Cardwell *et al.* (1978) show that high temperatures are generated by frictional heating only if a fault zone is relatively thin (i.e. <10 cm).

The relative ease with which an artificial pseudotachylyte has been generated using friction welding apparatus indicates that melting on fault planes should be commonplace. This does not appear to be the case, which suggests that the experiment failed to simulate the *mechanism* typical of seismogenic fault movement even though it occurred under similar velocity and rise time conditions.

In conclusion, it appears that pseudotachylyte is unlikely to be found in a wide seismogenic fault zone which last generated small earthquakes within anhydrous rock possessing abundant pore fluid. Conversely, pseudotachylyte is likely to be abundant in a narrow seismogenic fault zone which last generated large earthquakes in hydrous rock lacking pore fluid: apparently a relatively uncommon geological situation.

Acknowledgements—I am particularly grateful to David Nicholas of the Welding Institute, Cambridgeshire, for allowing me to load rock into friction welding apparatus and for his help and advice during the experiment. Initial ideas on the use of friction welding equipment for geological studies arose from discussions with Robert Wallach of the Department of Metallurgy and Materials Science, Cambridge. Graham Chinner kindly supplied the Skaergaard dolerite sample and Ken Pye provided valuable assistance with SEM photography and analysis. Talks with Geof King helped to clarify many of the ideas expressed in the paper.

REFERENCES

Abe, K. 1974a. Seismic displacement and ground motion near a fault: the Saitama earthquake of September 21, 1931. *J. geophys. Res.* **79**, 4393–4399.

Abe, K. 1974b. Fault parameters determined by near- and far-field data: the Wasaka Bay earthquake of March 26, 1963. *Bull. seism. Soc. Am.* **64**, 1369–1382.

Allen, A. R. 1979. Mechanism of frictional fusion in fault zones. *J. Struct. Geol.* **1**, 231–243.

Bowden, F. P. & Tabor, D. 1954. *The Friction and Lubrication of Solids. Part I.* Clarendon Press, Oxford.

Bowden, F. P. & Tabor, D. 1964. *The Friction and Lubrication of Solids. Part II.* Clarendon Press, Oxford.

Brace, W. F. & Byerlee, J. D. 1966. Stick-slip as a mechanism for earthquakes. *Science, Wash.* **153**, 990–992.

Byerlee, J. D. 1978. Friction of rocks. *Pure appl. Geophys.* **116**, 615–626.

Cardwell, R. K., Chinn, D. S., Moore, G. F. & Turcotte, D. L. 1978. Frictional heating on a fault zone with finite thickness. *Geophys. J. R. astr. Soc.* **52**, 525–530.

Carslaw, H. S. & Jaeger, J. C. 1959. *Conduction of Heat in Solids.* Clarendon Press, Oxford.

Chyi, K. L., Sinha, A. K. & Faulkner, G. J. 1985. Thermally induced strain and fracturing of minerals: implication of xenolith and melt interaction. *Abs. with Prog. geol. Soc. Am.* **17**, 546–547.

Deschamps, A. & King, G. C. P. 1983. The Campania–Lucania (southern Italy) earthquake of 23 November 1980. *Earth Planet. Sci. Lett.* **62**, 296–304.

Erismann, Th., Heuberger, H. & Preuss, E. 1977. Der Bimsstein von Kofels (Tirol), ein Bergsturtz "Frictionit". *Tschermaks Min. Petr. Mitt.* **24**, 67–119.

Friedman, M., Logan, J. M. & Rigert, J. A. 1974. Glass-indurated quartz gouge in sliding-friction experiments on sandstone. *Bull. geol. Soc. Am.* **85**, 937–942.

Grocott, J. 1981. Fracture geometry of pseudotachylyte generation zones: a study of shear fractures formed during seismic events. *J. Struct. Geol.* **3**, 169–178.

Heuberger, H., Masch, L., Preuss, E. & Schrocker, A. 1984. Quaternary landslides and rock fusion in central Nepal and in the Tyrolean Alps. *Mountain Res. Dev.* **4**, 345–362.

Higgins, M. W. 1971. Cataclastic rocks. *Prof. Pap. U.S. geol. Surv.* **687**.

Husseini, M. E. 1977. Energy balance for motion along a fault. *Geophys. J. R. astr. Soc.* **49**, 699–714.

Jaeger, J. C. 1943. Moving sources of heat and the temperature of sliding contacts. *J. Proc. New South Wales* **76**, 203–213.

Jeffreys, H. H. 1942. On the mechanics of faulting. *Geol. Mag.* **79**, 291–295.

Kanamori, H. 1972. Determination of effective tectonic stress associated with earthquake faulting, the Tottori earthquake of 1943. *Phys. Earth Planet. Interiors* **5**, 426–434.

Kanamori, H. 1973. Mode of strain release associated with major earthquakes in Japan. *A. Rev. Earth Planet. Sci.* **1**, 213–239.

Kanamori, H. & Stewart, D. S. 1976. Mode of strain release along the Gibbs Fracture Zone, Mid-Atlantic Ridge. *Phys. Earth Planet. Interiors* **11**, 312–332.

King, G. C. P. 1978. Geological faults: fracture, creep and strain. *Phil. Trans. R. Soc.* **A288**, 197–212.

Lachenbruch, A. H. 1980. Frictional heating, fluid pressure, and the resistance to fault motion. *J. geophys. Res.* **85**, 6097–6112.

Lachenbruch, A. H. & Sass, J. H. 1980. Heat flow and energetics of the San Andreas fault zone. *J. geophys. Res.* **85**, 6185–6223.

Maddock, P. 1981. Melt origin of fault-generated pseudotachylytes demonstrated by textures. *Geology* **11**, 105–108.

Masch, L., Wenk, H. R. & Preuss, E. 1985. Electron microscopy study of hyalomylonites—evidence for frictional melting in landslides. *Tectonophysics* **115**, 131–160.

McKenzie, D. P. & Brune, J. P. 1972. Melting on fault planes during large earthquakes. *Geophys. J. R. astr. Soc.* **29**, 65–78.

Philpotts, A. R. 1964. Origin of pseudotachylite. *Am. J. Sci.* **262**, 1008–1135.

Raase, P. 1974. Al and Ti contents of hornblendes, indicators of temperature and pressure of regional metamorphism. *Contr. Miner. Petrol.* **48**, 179–203.

Reynolds, D. L. 1954. Fluidization as a geological process, and its bearing on the problem of intrusive granites. *Am. J. Sci.* **252**, 577–613.

Scholz, C. H. 1980. Shear heating and the state of stress on faults. *J. geophys. Res.* **85**, 6174–6184.

Scholz, C. H. & Engelder, J. T. 1976. The role of asperity indentation and ploughing in rock friction—I. Asperity creep and stick-slip. *Int. J. Rock Mech. Min. Sci.* **13**, 149–154.

Scott, J. S. & Drever, H. I. 1953. Frictional fusion along a Himalayan thrust. *Proc. R. Soc. Edinb.* **65**, 121–142.

Shand, S. J. 1916. The pseudotachylite of Parijs (Orange Free State). *Q. Jl. geol. Soc. Lond.* **72**, 198–221.

Sibson, R. H. 1973. Interactions between temperature and pore-fluid pressure during earthquake faulting and a mechanism for partial or total stress relief. *Nature, Lond.* **243**, 66–68.

Sibson, R. H. 1975. Generation of pseudotachylyte by ancient seismic faulting. *Geophys. J. R. astr. Soc.* **43**, 775–794.

Sibson, R. H. 1980. Power dissipation and stress levels on faults in the upper crust. *J. geophys. Res.* **85**, 6239–6247.

Turcotte, D. L. & Schubert, G. 1973. Frictional heating of the descending lithosphere. *J. geophys. Res.* **78**, 5876–5886.

Wenk, H. R. 1978. Are pseudotachylites products of fracture or fusion? *Geology* **6**, 507–511.

APPENDIX

(1) The mean surface velocity, v, for abutted cylinder faces rotating in unison and off-axis (Fig. 8) is given by

$$v = d\pi \times R/60,$$

where d is the off-set (0.0015 m) and R the number of revolutions per minute (3000). Thus $v = 0.24\ \mathrm{m\ s^{-1}}$.

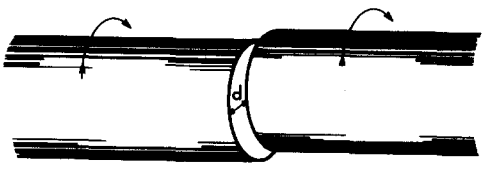

Fig. 8. Abutted cylinder faces rotating in unison, with off-set d.

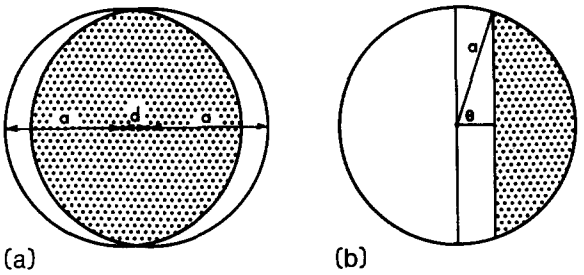

Fig. 9. (a) Contact surface area (stippled) between abutted cylinder faces of radius a. (b) Half the contact surface area.

(2) Contact surface area, A (Fig. 9a), for abutted cylinder faces juxtaposed off-axis is calculated by finding the area of the sector and subtracting the triangular areas to give the area of the chord (Fig. 9b) which represents $A/2$. This total contact area is given by

$$A = a^2\left(\theta - \frac{\sin 2\theta}{2}\right) \times 2 = 7.32 \text{ cm}^2,$$

where a is the radius of the cylinder (1.575 cm) and θ is in radians.

(3) There are a number of solutions for the generation of frictional heat at sliding contacts (e.g. Jaeger 1943, Carslaw & Jaeger 1959, pp. 266–270, Cardwell *et al.* 1978). For the purposes of this work an approximate determination of the temperature rise, ΔT, at the metadolerite interface is given by Bowden & Tabor (1954, pp. 33–35) for a cylinder moving under a normal load W at a surface speed v. It is assumed that all the frictional work is dissipated as heat and that the interface is receiving a fraction f of the total heat generated. Because the cylinder ends are in constant contact over the same area, $f = 1$, unlike the experiment of Bowden & Tabor where a cylinder is unidirectionally sliding over a flat surface where $f = 0.5$. Only heat loss by radiation is considered; heat loss by convection is ignored. The formula is as follows

$$\Delta T = \frac{f\mu Wgv}{J\pi a}\sqrt{\left(\frac{1}{2hKa}\right)} = 1400°\text{C},$$

where

f = fraction of total heat generated received by cylinder (1.0),
μ = static coefficient of friction for dolerite (0.75),
W = normal load (330,000 g),
g = acceleration due to gravity (981 cm s^{-2})
v = mean surface velocity (24 cm^{-1}). From (1) above,
J = mechanical equivalent of heat (4.8×10^7),
a = radius of contact surface area (1.53 cm). From (2) above,
h = heat transfer coefficient (0.02 cal cm^{-2}°C^{-1}),
K = thermal conductivity (0.005 cal cm^{-1} s^{-1} °C^{-1}).